Sawa Medical Journal
Reprint from
Vol.2 Issue.2 2026
ISSN : 3007-4738

Design and Synthesis of a Novel Propargylated Imidazole–Chalcone Hybrid and Its Preliminary Cytotoxic Evaluation Against MCF-7 Breast Cancer Cells

Abdulrhman Y. Khalifa

The General Directorate of Education in Muthanna, Samawah, Iraq

Article Information
Received: 1-6-2026
Accepted: 18-6-2026
Published: 1-7-2026

Abstract

Breast cancer remains one of the most common types of cancer affecting women worldwide, and despite the progress in treatment, there is still a continuous need to search for new compounds that may help in improving therapeutic outcomes. In this work, a series of imidazole–chalcone hybrid compounds **(PIM-1–PIM-5)** were synthesized through a simple multistep procedure. The synthetic route started with N-alkylation of imidazole **(1)** using propargyl bromide **(2)** to form a propargyl-substituted imidazole intermediate, followed by formylation at the 4-position of the imidazole ring. The resulting aldehyde was then subjected to Claisen–Schmidt condensation with different substituted acetophenones **(3)** to afford the target chalcone derivatives. The cytotoxic activity of the synthesized compounds was evaluated against MCF-7 using the MTT assay. The results showed that the compounds exhibited different levels of growth inhibition depending on the substituent on the aromatic ring. Among the tested derivatives, PIM-4 displayed the highest activity with an IC_{50} value of about 7.4 μM, while the other compounds showed moderate to lower activity. The structures of the synthesized compounds were confirmed using spectroscopic techniques including FT-IR, ^{1}H NMR and ^{13}C NMR.

Keywords: imidazole–chalcone hybrid, breast cancer, MCF-7 cells.

Introduction

Breast cancer is one of the most common cancers among women worldwide and a leading cause of cancer-related deaths. This makes the looking for new cure strategies crucial in the fields of medicinal-chemistry and medical research (Xiong et al., 2025, Kim et al., 2025 and Godiveau, et al., 2025). Recent studies refer that the genetic and biological-diversity of this disease makes developing effective treatments an ongoing challenge. Therefore researchers continue to looking for new compounds that can help to inhibit the

growth of cancer cells with more effectively (Shokoohi et al., 2025, Xiong et al., 2025, Bai, et al., 2025 and Garg et al, 2025).

However the heterocycles have significant role in the synthesis of pharmaceutical agents (Kabir et al., 2022). Between these rings is the imidazole ring which is found in many well-known bio-molecules and pharmaceutical compounds (Shalini et al., 2010). Derivatives of imidazole have been reported to exhibit various biological-activities such as antibacterial (Bayar et al., 2023), antifungal (Ellis et al., 1964 and Peçe et al, 2026) and antitumor-activity (Kumar et al., 2023) which making them important chemical building blocks in the design of new drugs (Youssef et al., 2026, Golcienė et al, 2026 and Kamurthy et al, 2025).

Furthermore chalcone compounds constitute significant chemical entities in medicinal-chemistry (Zhuang et al., 2017 and Rammohan et al, 2020). They are characterized by the presence of an α,β-unsaturated carbonyl system which gives them various biological properties (Maydt et al., 2013). Numerous studies have confirmed that chalcone derivatives possess antitumor-activity and can inhibit the growth of various cancer cell lines that including breast cancer cells (Ouyang et al., 2021 and Yang et al, 2023). Recent studies also indicated that these compounds can target different intracellular proteins such as tubulin or certain enzymes involved in cell-division (Saleem et al., 2026, Zheng et al 2026 and Yan et al, 2025).

In recent years many studies have focused on the design of hybrid molecules and a strategy that combines multiple active chemical components into a single molecule to obtain compounds with enhanced biological-activity (Bérubé et al., 2016). Some studies have shown that combining an imidazole ring with a chalcone structure can lead to compounds with anticancer activity by influencing processes such as the inhibition of microtubule formation or the induction of apoptosis (Oskuei et al., 2021).

Accordingly, this research designed and synthesized a series of hybrid compounds combining imidazole and chalcone in a single molecule, with the addition of a propargyl group as a substituent that can influence the electronic and structural properties of the compound. The central idea of this work is to explore whether combining these chemical structures can lead to novel compounds with initial activity against breast cancer cells. Therefore, this work aims to prepare several imidazole-chalcone hybrid derivatives and evaluate their cytotoxic activity against MCF-7 cells using a cell viability assay, in order to gain an initial understanding of their ability to inhibit the growth of these cells and their potential for future development as candidate compounds in anticancer research.

Experimental

2.1. Materials and Methods

All chemicals used were of analytical grade and were obtained from Sigma Aldrich. Reaction progress was monitored by thin-layer chromatography (TLC) on silica gel plates and visualized under UV light. Melting points were determined using a digital melting point apparatus and are uncorrected. Infrared spectra were recorded using KBr pellets and expressed in cm^{-1}. ^{1}H NMR and ^{13}C NMR spectra were recorded in DMSO-d_6 using tetramethylsilane (TMS) as internal standard. Chemical shifts (δ) are reported in ppm. High-resolution mass spectra (HRMS) were obtained using electrospray ionization (ESI) techniques.

2.2. Synthesis

2.2.1. Synthesis of 1-(prop-2-yn-1-yl)-1H-imidazole (PI)

In a 100 mL flask, imidazole (6.80 g, 0.10 mol, 1.0 eq) and anhydrous K_2CO_3 (13.8 g, 0.10 mol, 1.0 eq) were added in dry DMF (50 mL) under a nitrogen atmosphere. The mixture was stirred for 15 minutes at room temperature, then propargyl bromide (80% in toluene, 12.5 g, 0.105 mol, 1.05 eq) was added drip-over 20 minutes, and the reaction was raised to 40°C with stirring for 8 hours (TLC monitoring, hexane/EtOAc 7:3). After the reaction was completed, the mixture was poured into 100 mL of cold water and extracted in three batches of ethyl acetate (3 x 50 mL). The organic phase was dried with Na_2SO_4 and concentrated under low pressure. The product was then purified by silica column chromatography to give compound (PI) (March et al., 1985) in a yield of 78–85% as a colorless oily substance. Obtained as a pale yellow liquid; b.p.: 198–200 °C. IR (KBr, ν_max, cm^{-1}): 3305 (≡C–H), 3130 (Ar–H), 2105 (C≡C), 1568 (C=N), 1450 (C=C), 1250 (C–N). ^{1}H-NMR (400 MHz, $CDCl_3$, δ ppm): 7.55 (1H, dd, *J* = 1.8, 1.5 Hz, imidazole-H), 7.22 (1H, dd, *J* = 3.7, 1.5 Hz, imidazole-H), 6.87 (1H, dd, *J* = 3.7, 1.8 Hz, imidazole-H), 4.58 (s, 2H, N–CH_2), 2.78 (s, 1H, ≡C–H). ^{13}C-NMR (100 MHz, $CDCl_3$, δ ppm): 138 (C=N), 129.5 (CH-imidazole), 120.1 (CH-imidazole), 77.1 (C≡C), 76.5 (C≡C), 50.4 (N–CH_2).

2.2.2. Synthesis of 1-(prop-2-yn-1-yl)-1H-imidazole-4-carbaldehyde (PIMC)

In an ice bath (0–5°C), $POCl_3$ (9.2 mL, 0.10 mol) was slowly added to DMF (20 mL) with stirring to form the active complex. After 15 minutes, compound (PI) (10.8 g, 0.09 mol) was gradually added, and the reaction was then raised to 80°C and stirred for 6 hours. After cooling, the mixture was poured onto 150 g of crushed ice and the pH was adjusted to 7 using 10% NaOH. The solid product precipitated, was filtered, washed with cold water, and recrystallized from ethanol to give compound PIMC (Larock et al., 1989) with a yield of 70–75%.Obtained as a pale yellow crystalline solid. m.p.: 142–144 °C. IR (KBr, ν_max, cm^{-1}): 3290 (≡C–H), 3125 (Ar–H), 2102 (C≡C), 1685 (CHO, C=O), 1565 (C=N), 1458 (C=C), 1245 (C–N). ^{1}H-NMR (400 MHz, DMSO-d_6, δ ppm): 9.77 (s, 1H, CHO), 7.78 (s, 1H, imidazole-H), 7.54 (d, 1H, *J* = 1.6 Hz, imidazole-H), 4.94 (s, 2H, N–CH_2), 2.78 (s, 1H, ≡C–H). ^{13}C-NMR (100 MHz, DMSO-d_6, δ ppm): 179.5 (CHO), 136.5 (C=N), 135.6 (imidazole C), 124.7 (CH-imidazole), 77.1 (C≡C), 76.5 (C≡C), 50.4 (N–CH_2).

2.2.3. Synthesis of (E)-1-(4-substituted phenyl)-3-[1-(prop-2-yn-1-yl)-1H-imidazol-4-yl]prop-2-en-1-one (PIM-1 – PIM-5)

In a 100 mL flask, compound PIMC (5.0 g, 0.03 mol) and 4-substituted acetophenone (0.03 mol) were dissolved in absolute ethanol (40 mL), and NaOH solution (10 mL, 20%) was added by drip infusion with stirring at room temperature for 24 hours. The reaction progress was monitored by TLC (EtOAc/hexane 3:7). After the reaction was completed, the mixture was poured into 200 mL of ice-cold water, and the pH was adjusted to 5 using dilute HCl. The compound precipitated, was filtered, washed with water, and recrystallized from ethanol to give the final chalcone derivatives (PIM-1 – PIM-5) (Liu et al., 2024) as an (E)-isomer structure with a yield of 74–81% and a melting point of 168–198°C.

2.2.3.1. (2E)-1-(4-hydroxyphenyl)-3-[1-(prop-2-yn-1-yl)-1H-imidazol-4-yl]prop-2-en-1-one (PIM-1).

Yield: 78%; m.p. 182–184 °C. IR (KBr, cm^{-1}): 3295 (≡C–H), 3215 (O–H), 3110 (Ar–H), 2108 (C≡C), 1658 (C=O), 1602 (C=C), 1515 (C=N), 1265 (C–O). ^{1}H-NMR (400 MHz, DMSO-d_6, δ ppm): 9.98 (s, 1H, OH), 7.77 (d, 1H, *J* = 1.8 Hz imidazole-H), 7.60 (d, J = 8.2 Hz, 2H, Ar-H), 7.45 (d, 1H, *J* = 1.8 Hz, imidazole-H), 7.16 (d, J = 18.1 Hz, 1H, CH=CH), 6.99 (d, J = 8.2 Hz, 2H, Ar-H), 6.64 (d, J = 18.1 Hz,

1H, CH=CH), 4.97 (s, 2H, N–CH_2), 2.78 (s, 1H, ≡C–H). ^{13}C-NMR (100 MHz, DMSO-d_6, δ ppm): 188.3 (C=O), 160.9 (Ar-C–OH), 136.5, 136.1, 124.7 (imidazole C), 115.9, 131.4, 136.1 (aromatic carbons), 128.2 (=CH), 119.1 (=CH), 77.1 (C≡C), 76.5 (C≡C), 50.4 (N–CH_2).

2.2.3.2. (2E)-1-(4-methoxyphenyl)-3-[1-(prop-2-yn-1-yl)-1H-imidazol-4-yl]prop-2-en-1-one (PIM-2).

Yield: 81%; m.p. 168–170 °C. IR (KBr, cm^{-1}): 3292 (≡C–H), 3105 (Ar–H), 2105 (C≡C), 1656 (C=O), 1600 (C=C), 1512 (C=N), 1248 (Ar–O–CH_3). ^{1}H-NMR (400 MHz, DMSO-d_6, δ ppm): 7.96 (d, J = 8.3 Hz, 2H, Ar-H), 7.77 (d, 1H, *J* = 1.8 Hz imidazole-H), 7.45 (d, 1H, *J* = 1.8 Hz, imidazole-H), 7.16 (d, J = 18.1 Hz, 1H, CH=CH), 7.05 (d, J = 8.3 Hz, 2H, Ar-H), 6.64 (d, J = 18.1 Hz, 1H, CH=CH), 4.97 (s, 2H, N–CH_2), 3.86 (s, 3H, OCH_3), 2.78 (s, 1H, ≡C–H). ^{13}C-NMR (100 MHz, DMSO-d_6, δ ppm): 188.27 (C=O), 162.4 (Ar-C–O), 136.5, 136.1, 124.7 (imidazole C), 113.8, 130.7, 130.9, 136.1 (aromatic carbons), 128.2 (=CH), 119.1 (=CH), 77.08 (C≡C), 76.48 (C≡C), 55.3 (OCH_3), 50.4 (N–CH_2).

2.2.3.3. (2E)-1-(4-fluorophenyl)-3-[1-(prop-2-yn-1-yl)-1H-imidazol-4-yl]prop-2-en-1-one (PIM-3).

Yield: 76%; m.p. 174–176 °C. IR (KBr, cm^{-1}): 3290 (≡C–H), 3108 (Ar–H), 2104 (C≡C), 1660 (C=O), 1603 (C=C), 1508 (C=N), 1115 (C–F). ^{1}H-NMR (400 MHz, DMSO-d_6, δ ppm): 7.69 (d, J = 8.3 Hz, 2H, Ar-H), 7.79 (d, 1H, *J* = 1.8 Hz imidazole-H), 7.45 (d, 1H, *J* = 1.8 Hz, imidazole-H), 7.16 (d, J = 18.1 Hz, 1H, CH=CH), 7.37 (d, J = 8.3 Hz, 2H, Ar-H), 6.66 (d, J = 18.1 Hz, 1H, CH=CH), 4.99 (s, 2H, N–CH_2), 2.8 (s, 1H, ≡C–H). ^{13}C-NMR (100 MHz, DMSO-d_6, δ ppm): 188.29 (C=O), 164.9 (Ar-C–F), 136.5, 136.1, 124.7 (imidazole C), 115.8, 131.07, 134.9 (aromatic carbons), 128.2 (=CH), 119.1 (=CH), 77.07 (C≡C), 76.47 (C≡C), 50.37 (N–CH_2).

2.2.3.4. (2E)-1-(4-nitrophenyl)-3-[1-(prop-2-yn-1-yl)-1H-imidazol-4-yl]prop-2-en-1-one (PIM-4).

Yield: 74%; m.p. 196–198 °C. IR (KBr, cm^{-1}): 3291 (≡C–H), 3112 (Ar–H), 2106 (C≡C), 1662 (C=O), 1605 (C=C), 1520 and 1345 (NO_2), 1510 (C=N).

^{1}H-NMR (400 MHz, DMSO-d_6, δ ppm): 8.17 (d, J = 8.3 Hz, 2H, Ar-H), 7.78 (d, 1H, *J* = 1.8 Hz imidazole-H), 7.47 (d, 1H, *J* = 1.8 Hz, imidazole-H), 7.2 (d, J = 17.2 Hz, 1H, CH=CH), 7.9 (d, J = 8.3 Hz, 2H, Ar-H), 6.71 (d, J = 17.2 Hz, 1H, CH=CH), 4.96 (s, 2H, N–CH_2), 2.76 (s, 1H, ≡C–H). ^{13}C-NMR (100 MHz, DMSO-d_6, δ ppm): 188.28 (C=O), 149.4 (Ar-C– NO_2), 136.5, 136.1, 124.7 (imidazole C), 123.9, 129.2, 134.9 (aromatic carbons), 128.2 (=CH), 119.1 (=CH), 77.08 (C≡C), 76.48 (C≡C), 50.39 (N–CH_2).

2.2.3.5. (2E)-1-(4-chlorophenyl)-3-[1-(prop-2-yn-1-yl)-1H-imidazol-4-yl]prop-2-en-1-one (PIM-5).

Yield: 79%; m.p. 180–182 °C. IR (KBr, cm^{-1}): 3290 (≡C–H), 3106 (Ar–H), 2104 (C≡C), 1659 (C=O), 1602 (C=C), 1506 (C=N), 1090 (C–Cl). ^{1}H-NMR (400 MHz, DMSO-d_6, δ ppm): 7.74 (d, J = 8.7 Hz, 2H, Ar-H), 7.77 (d, 1H, *J* = 1.8 Hz imidazole-H), 7.45 (d, 1H, *J* = 1.8 Hz, imidazole-H), 7.16 (d, J = 18 Hz, 1H, CH=CH), 7.49 (d, J = 8.7 Hz, 2H, Ar-H), 6.64 (d, J = 18 Hz, 1H, CH=CH), 4.95 (s, 2H, N–CH_2), 2.77 (s, 1H, ≡C–H). ^{13}C-NMR (100 MHz, DMSO-d_6, δ ppm): 188.27 (C=O), 138.5 (Ar-C– Cl), 136.5, 136.1, 124.7 (imidazole C), 129.2, 129.9 134.9 (aromatic carbons), 128.2 (=CH), 119.1 (=CH), 77.06 (C≡C), 76.46 (C≡C), 50.37 (N–CH_2).

2.3. **Cytotoxicity Assays (MTT assay)**

The cytotoxic activity of the prepared compounds (PIM-1–PIM-5) was evaluated using the human breast cancer cell line MCF-7 with the MTT assay. Cells were seeded in 96-well dishes at an approximate density of 1×10^4 cells per well using Dulbecco's Modified Eagle Medium supplemented with 10% fetal bovine serum and 1% antibiotics. The cells were incubated at 37°C in a 5% CO_2 incubator for 24 hours to allow adhesion and growth. Subsequently, the cells were treated with different concentrations of the prepared

compounds (0.1, 1, 10, 25, 50, and 100 µM) for 48 hours. After incubation, MTT solution was added to each well to a final concentration of 0.5 mg/mL, and the dishes were incubated for 4 hours. The medium was then removed, and DMSO was added to dissolve the resulting formazan crystals. Absorbance was measured at a wavelength of 570 nm using a microplate reader (Bahuguna et al., 2017). The cell viability ratio was calculated compared to untreated cells, and then the IC_{50} value was calculated for each compound.

Results

3.1.Identification of synthesized compounds:

The synthesized compounds were successfully diagnosed and confirmed using (FT-IR), (^{1}H-NMR), (^{13}C-NMR), and mass spectrometry.

3.1.1. The FT-IR spectrum of the compounds (PI, PIMC and PIM-1-5) shows the absorption bands as illustrated in **Table 1** and **Figures (1-7).**

Table 2. FT-IR spectral data (cm^{-1}) of the synthesized compounds (PI, PIMC and PIM-1- PIM-5).

Com.	≡C–H	Ar–H	C≡C	C=O / CHO	C=N	C=C	Other functional groups
PI	3305	3130	2105	-	1586	1450	1250 (C-N)
PIMC	3290	3125	2102	1685 (CHO)	1565	1458	1245 (C-N)
PIM-1	3295	3110	2108	1658	1515	1602	3215 (OH)
PIM-2	3292	3105	2105	1656	1512	1600	1248 (O-CH3)
PIM-3	3290	3108	2104	1660	1508	1603	1115 (C-F)
PIM-4	3291	3112	2106	1662	1510	1605	1520, 1345 (NO2)
PIM-5	3290	3106	2104	1659	1506	1602	1090 (C-Cl)

3.1.2. ^{1}H-NMR spectrum of the synthesized compounds (PI, PIMC, and PIM-1- PIM-5) is shown in **Table 2** and **Figures (8-14).**

Table 2. ^{1}H-NMR spectral data (δ ppm) of the synthesized compounds (PI, PIMC and PIM-1- PIM-5).

Com.	Imidazole-H	Ar-H	CH=CH	N-CH_2	≡C-H	Other groups
PI	7.55, 7.22, 6.87	—	—	4.58	2.78	—
PIMC	7.78, 7.54	—	—	4.94	2.78	9.77 (CHO)
PIM-1	7.77, 7.45	7.60, 6.99	7.16, 6.64	4.97	2.78	9.98 (OH)
PIM-2	7.77, 7.45	7.96, 7.05	7.16, 6.64	4.97	2.78	3.86 (OCH_3)
PIM-3	7.79, 7.45	7.69, 7.37	7.16, 6.66	4.99	2.8	—
PIM-4	7.78, 7.47	8.17, 7.90	7.20, 6.71	4.96	2.76	—

PIM-5	7.77, 7.45	7.74, 7.49	7.16, 6.64	4.95	2.77	—

3.1.3. ^{13}C-NMR spectrum of the synthesized compounds (PI, PIMC, and PIM-1- PIM-5) is shown in **Table 3** and **Figures (15-21).**

Table 3. ^{13}C-NMR spectral data (δ ppm) of the synthesized compounds (PI, PIMC and PIM-1- PIM-5).

Com.	C=N / C=O	Imidazole C / CH	Aromatic carbons	C≡C	C=C	N-CH_2	Other groups
PI	138 (C=N)	129.5, 120.1	—	77.1, 76.5	—	50.4	—
PIMC	136.5 (C=N) 179.5 (CHO)	135.6, 124.7	—	77.1, 76.5	—	50.4	—
PIM-1	188.3 (C=O)	136.5, 136.1, 124.7	115.9, 131.4, 136.1	77.1, 76.5	128.2, 119.1	50.4	160.9 (Ar–OH)
PIM-2	188.27 (C=O)	136.5, 136.1, 124.7	113.8, 130.7, 130.9, 136.1	77.08, 76.48	128.2, 119.1	55.3, 50.4	162.4 (Ar–OCH_3)
PIM-3	188.29 (C=O)	136.5, 136.1, 124.7	115.8, 131.07, 134.9	77.07, 76.47	128.2, 119.1	50.37	164.9 (Ar–F)
PIM-4	188.28 (C=O)	136.5, 136.1, 124.7	123.9, 129.2, 134.9	77.08, 76.48	128.2, 119.1	50.39	149.4 (NO_2)
PIM-5	188.27 (C=O)	136.5, 136.1, 124.7	129.2, 129.9, 134.9	77.06, 76.46	128.2, 119.1	50.37	138.5 (C–Cl)

The spectra of all synthesized compounds (PI, PIMC and PIM-1- PIM-5) are shown in the Appendix (Figures 1–21).

3.2. Anticancer Activity

The cytotoxic activity of the synthesized compounds (PIM-1-5) against the human breast cancer cell line MCF-7 was evaluated using the MTT assay. All results are summarized in **Table 4**, **Table 5** and **Figure 22** .

Table 4: Percentage inhibition of cell proliferation of the synthesized imidazole-chalcone derivatives (PIM-1–PIM-5) against MCF-7.

Concentration (µM)	Compounds				
	PMI-1	**PMI-2**	**PMI-3**	**PMI-4**	**PMI-5**
0.1	3	4	6	8	5
1	8	12	18	25	20
10	28	35	42	55	48

25	52	60	68	78	72
50	71	79	84	90	86
100	88	92	95	97	96

Table 5: IC_{50} values of synthesized imidazole-chalcone derivatives (PIM-1–PIM-5) against MCF-7 cells determined by the MTT assay.

Compound	Substituent	IC_{50} (µM)
PMI-1	4-OH	18.6 ± 0.9
PMI-2	4-OCH_3	14.2 ± 0.7
PMI-3	4-F	11.8 ± 0.5
PMI-4	4-NO_2	**7.4 ± 0.3**
PMI-5	4-Cl	9.6 ± 0.4

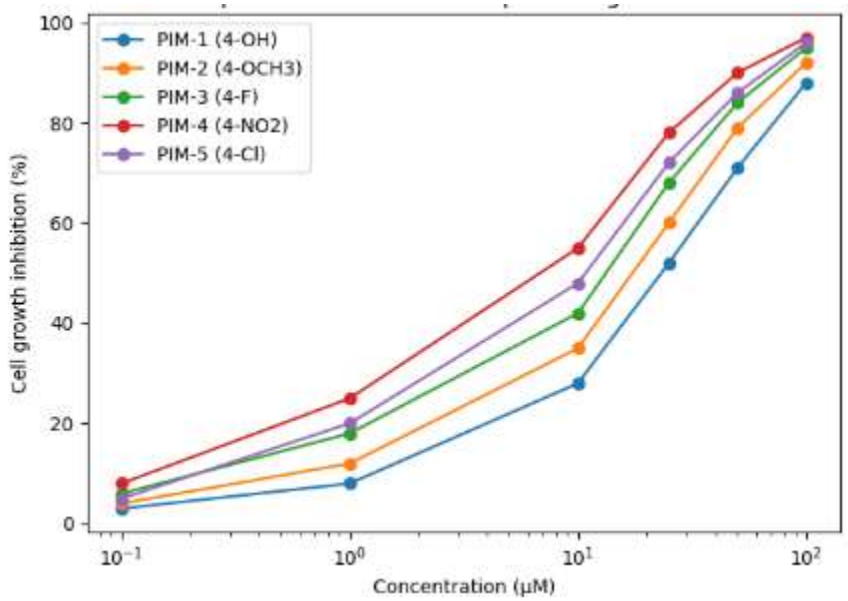

Figure 22: Dose–response curves of synthesized imidazole-chalcone derivatives (PIM-1–PIM-5) against MCF-7 determined by MTT assay after 48 h treatment.

4. Discussion

4.1. Synthesis

In this study as shown in (Scheme 1), the synthesis of the intermediate compound (PI) was initiated by the reaction of imidazole (1) with propargyl bromide (2) in the presence of potassium carbonate as a base in a suitable organic medium. This reaction led to the alkylation of the nitrogen atom in the imidazole ring and the formation of the compound 1-(prop-2-yn-1-yl)-1H-imidazole (PI). Spectroscopic data confirmed the success of this step, as the IR spectrum (**Table 1 and Fig. 1**) showed a characteristic band at approximately 3305 cm^{-1} due to the ≡C–H terminal vibration, in addition to a band at approximately 2105 cm^{-1} due to the C≡C triple bond, while other bands belonging to the imidazole heterocyclic ring appeared in the 1586 cm^{-1} (Wong, 2015). In **Table 2** and **Figure 8,** the ^{1}H-NMR spectrum showed the imidazole

ring protons in the aromatic domain between 6.87 and 7.55 ppm, while a two-score signal appeared at approximately 4.58 ppm, attributed to the N–CH_2 group protons attached to the properyl chain. A three-score signal was also observed near 2.78 ppm, attributed to the terminal proton of the triple bond. In **Table 3** and **Figure 15,** the ^{13}C NMR spectrum confirmed the presence of the triple bond carbon at approximately 76.5 and 77.1 ppm and the CH_2 group carbon at approximately 50.4 ppm, indicating the formation of the desired compound (PI) (Pavia, et al., 2015).

Subsequently, the formalization reaction was performed using the Vilsmeier–Haack reagent obtained from the reaction of DMF with $POCl_3$. An aldehyde group was introduced at the fourth position of the imidazole ring for compound (PI) to form the compound 1-(prop-2-yn-1-yl)-1H-imidazole-4-carbaldehyde (PIMC). In **Table 1** and **Figure 2**, the IR spectrum confirmed the formation of this compound by showing a strong band at approximately 1685 cm^{-1} belonging to the aldehyde carbonyl group, while the triple bond band remained unchanged at approximately 2102 cm^{-1}, indicating that the properyl group was unaffected by the reaction. In **Table 2** and **Figure 9,** the ^1H NMR spectrum also showed a distinct single signal for the aldehyde proton at approximately 9.7 ppm, a characteristic value for the CHO proton, in addition to the continued presence of imidazole protons in the aromatic domain. In **Table 3** and **Figure 16,** the ^{13}C NMR spectrum showed a signal at approximately 179.5 ppm belonging to the aldehyde carbon, along with signals for the carbons of the triple bond and the heterocyclic ring.

In the final step, this aldehyde (PIMC) was used as a substrate for the synthesis of a series of imidazole-chalcone compounds (PIM-1 – PIM-5) via Claisen–Schmidt condensation with several para-substituted acetophenone derivatives (3). 4-hydroxyacetophenone, 4-methoxyacetophenone, 4-fluoroacetophenone, 4-nitroacetophenone, and 4-chloroacetophenone were used to obtain five new imidazole-chalcone compounds (PIM-1 – PIM-5). The reaction took place in an ethanolic medium with sodium hydroxide as the base. Condensation occurred between the aldehyde and ketone groups, forming a conjugated system of the α,β-unsaturated ketone type characteristic of chalcones. The different spectra supported the formation of these compounds (PIM-1 – PIM-5). In **Table 1** and **Figures (3-7),** the IR spectrum, a strong band appeared in the 1656–1662 cm^{-1} range, belonging to the unsaturated carbonyl group C=O, in addition to a band at approximately 1450–1605 cm^{-1} belonging to the conjugated C=C bond. The C≡C triple bond signal remained at approximately 2100 cm^{-1}, indicating the persistence of the propargil group in the final structure of the compounds (PIM-1–PIM-5). In **Table 2** and **Figures (10-14),** the ^1H NMR spectrum showed two distinct doublet signals at approximately 6.64–7.2 ppm belonging to the double bond protons in the chalcon system, with a large coupling value ($J \approx 18$ Hz), indicating that the double bond spatial configuration is of the E-configuration type. The aromatic proton signals of the phenyl rings appeared in the 6.99–8.17 ppm range, depending on the nature of the substituent group in the ring. In the case of the compound (PIM-1) containing the hydroxyl group, the OH proton signal appeared at approximately 9.77 ppm, while the OCH_3 signal in the second compound (PIM-2) appeared at around 3.86 ppm. In **Table 3** and **Figure (17-21),** ^{13}C NMR spectra showed distinct carbonyl carbon signals at around 188 ppm, in addition to C=C conjugate carbons in the 119–128 ppm range, while the triple bond carbons (C≡C) remained in the 76.47–77.1 ppm range. This may give these compounds (PIM-1–PIM-5) distinctive biological properties due to the presence of the conjugate system and the different substitution groups on the aromatic ring.

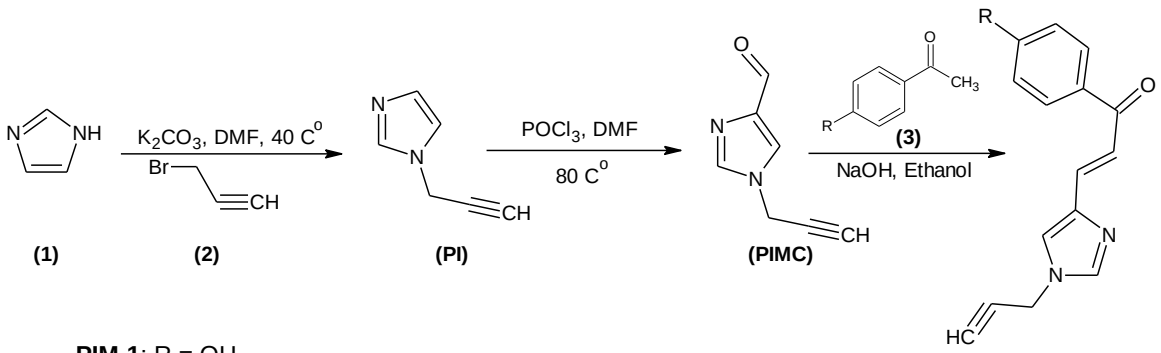

PIM-1: R = OH
PIM-2: R = OCH_3
PIM-3: R = F
PIM-4: R = NO_2
PIM-5: R = Cl

Scheme 1: Synthesis of Imidazole-Chalcone Derivatives (PIM-1–PIM-5)**.**

4.2. Anticancer Study

The activity of cytotoxic of the prepared compounds (PIM-1-PIM-5) against human MCF-7 breast-cancer cells was evaluated using the MTT assay. Cells were treated with different concentrations of the compounds (0.1–100 µM) for 48 hours and after which cell viability was measured and compared to untreated cells. As shown in (Table 4) all compounds exhibited progressive increase in cell growth inhibition with increasing concentration, reflecting a clear dose-to-biological relationship. At the lowest concentration (0.1 µM), inhibition rates were very limited which ranging from 3% to 8%, while these values increased significantly at higher concentrations. At a concentration of 10 µM the cell growth inhibition rates ranged from 28% to 55%, depending on the compound which indicating significant differences in cytotoxic activity between the various compounds. As shown in (Fig. 22) which depicts the dose-response curves and all compounds exhibited dose-dependent behavior with cell growth-inhibition gradually increasing with increasing compound concentration. The figure 1show that compound PIM-4 has the steepest curve compared to the other compounds and indicating its higher activity against MCF-7 cells. According to the data shown in (Table 4), compound PIM-4 containing nitro group confirmed the highest cytotoxic activity with cell growth inhibition reaching approximately 55% at concentration of 10 µM and increasing to approximately 78% at concentration of 25 µM. Inhibition reached approximately 97% at concentration of 100 µM. These results indicate that this compound has the highest activity within this series. In contrast compound PIM-1, containing hydroxy group showed the lowest relative activity among the studied compounds, with cell inhibition not exceeding approximately 28% at a concentration of 10 µM, as shown in (Table 4). This indicates that higher concentrations are required for this compound to achieve the same level of activity as the other compounds. Compounds PIM-3 and PIM-5 showed relatively moderate activity with cell inhibition rate reaching approximately 42% and 48% respectively at concentration of 10 µM.

Looking at the IC_{50} values shown in (Table 5), the picture becomes clearer. Compound PIM-4 was the most active with the IC_{50} value of approximately 7.4 µM meaning it required relatively low concentration to inhibit half of the cell growth. In contrast, compound PIM-1 was the least active, with an IC_{50} value of approximately 18.6 µM. The other compounds, such as PIM-3 and PIM-5, showed moderate activity, with

IC_{50} values roughly between these two extremes. It is also clear that the type of group on the aromatic ring has a significant impact on toxic activity. Compounds with electron-withdrawing groups, such as NO_2, Cl, and F, appeared more active than those with electron-donating groups, such as OH and OCH_3. This can be explained by the fact that these groups may influence the nature of the conjugated system in the chalcone structure, perhaps making the compound more capable of interacting with certain intracellular molecules. Overall, the results indicate that this series of compounds exhibits significant activity against MCF-7 cells, with PIM-4 showing a clear advantage over the other compounds. Therefore, this particular compound may be a promising candidate for further biological studies in the future.

Conclusion

In this work, a series of imidazole–chalcone hybrid compounds (PIM-1–PIM-5) were successfully synthesized through a multistep synthetic route starting from propargyl-substituted imidazole followed by Claisen–Schmidt condensation to form the chalcone derivatives. The cytotoxic activity of the obtained compounds was evaluated against the human breast cancer cell line MCF-7 using the MTT assay. The results showed that the synthesized compounds displayed different levels of activity, where PIM-4 exhibited the highest cytotoxic effect compared with the other derivatives. In general, the results suggest that combining imidazole and chalcone frameworks in a single molecule may provide compounds with promising biological activity. These findings may serve as a starting point for further studies aimed at improving the biological potential of this type of compounds.

References

Bahuguna, A., Khan, I., Bajpai, V. K., & Kang, S. C. (2017). MTT assay to evaluate the cytotoxic potential of a drug. *Bangladesh Journal of Pharmacology*, *12*(2), Online-Apr.

Bai, J., Gao, Y., & Zhang, G. (2025). The treatment of breast cancer in the era of precision medicine. *Cancer biology & medicine*, *22*(4), 322-347.

Bayar, I., & Akkoc, S. (2023). Antibacterial activities of imidazole-based compounds (a review). *Russian Journal of Organic Chemistry*, *59*(Suppl 1), S7-S19.

Bérubé, G. (2016). An overview of molecular hybrids in drug discovery. *Expert opinion on drug discovery*, *11*(3), 281-305.

Ellis, G. P., Epstein, C., Fitzmaurice, C., Golberg, L., & Lord, G. H. (1964). Antifungal activity of some imidazole derivatives. *Journal of Pharmacy and Pharmacology*, *16*(6), 400-407.

Garg, P., Ramisetty, S., Nair, M., Kulkarni, P., Horne, D., Salgia, R., & Singhal, S. S. (2025). Strategic advancements in targeting the PI3K/AKT/mTOR pathway for Breast cancer therapy. *Biochemical Pharmacology*, *236*, 116850.

Godiveau, M., Jahanmohan, J. P., Abrial, C., & Durando, X. (2025). Chemotherapy-induced peripheral neuropathy in patients with breast cancer treated with taxanes. *Oncology Letters*, *30*(5), 508.

Golcienė, B., Maciejewska, N., Kallingal, A., Sapijanskaitė-Banevič, B., Stasevych, M., & Mickevičius, V. (2026). Imidazole-2-thione derivatives as new selective anticancer agents with anti-metastatic properties: synthesis and pharmacological evaluation. *Journal of Enzyme Inhibition and Medicinal Chemistry*, *41*(1), 2607820.

Kabir, E., & Uzzaman, M. (2022). A review on biological and medicinal impact of heterocyclic compounds. *Results in Chemistry*, *4*, 100606.

Kim, J., & Munster, P. N. (2025). Estrogens and breast cancer. *Annals of Oncology*, *36*(2), 134-148.

Kumar, N., & Goel, N. (2023). Recent development of imidazole derivatives as potential anticancer agents. *Physical Sciences Reviews*, *8*(10), 2903-2941.

Larock, R. C. (1989). *Comprehensive organic transformations* (pp. 411-415). New York, NY, USA: Mcgraw-Hill.

Liu, Z., Yang, Z., & Ablise, M. (2024). Design and synthesis of novel imidazole-chalcone derivatives as microtubule protein polymerization inhibitors to treat cervical cancer and reverse cisplatin resistance. *Bioorganic Chemistry*, *147*, 107310.

March, J. (1985). *Advanced organic chemistry: reactions, mechanisms, and structure* (Vol. 344). New York: Wiley.

Maydt, D., De Spirt, S., Muschelknautz, C., Stahl, W., & Müller, T. J. (2013). Chemical reactivity and biological activity of chalcones and other α, β-unsaturated carbonyl compounds. *Xenobiotica*, *43*(8), 711-718.

Oskuei, S. R., Mirzaei, S., Jafari-Nik, M. R., Hadizadeh, F., Eisvand, F., Mosaffa, F., & Ghodsi, R. (2021). Design, synthesis and biological evaluation of novel imidazole-chalcone derivatives as potential anticancer agents and tubulin polymerization inhibitors. *Bioorganic Chemistry*, *112*, 104904.

Ouyang, Y., Li, J., Chen, X., Fu, X., Sun, S., & Wu, Q. (2021). Chalcone derivatives: role in anticancer therapy. *Biomolecules*, *11*(6), 894.

Pavia, D. L., Lampman, G. M., Kriz, G. S., & Vyvyan, J. R. Introduction to spectroscopy 5th ed. United States: Cengage Learning; 2015.

Peçe, S., Osmaniye, D., Sağlık Özkan, B. N., Levent, S., Ozkay, Y., & Kaplancıklı, Z. A. (2026). Design, synthesis and investigation of new imidazole derivatives with biological activities and antifungal effects. *Journal of Biomolecular Structure and Dynamics*, *44*(2), 952-966.

PM, K., Kamurthy, H., Pal, R., PM, G. S., Gugal, P., M, S., & CM, S. (2025). Advancement of Imidazole Derivatives as Potential Anticancer Agents: Insight Into Structural Activity Relationship (SAR) Studies. *ChemistrySelect*, *10*(46), e02442.

Rammohan, A., Reddy, J. S., Sravya, G., Rao, C. N., & Zyryanov, G. V. (2020). Chalcone synthesis, properties and medicinal applications: a review. *Environmental Chemistry Letters*, *18*(2), 433-458.

Saleem, B. A., Qurtam, A. A., Ahmed, M., Al-Aouadi, R. F. A., Alrikabi, A. A. A., Hetta, H. F., ... & Farhan, S. M. (2026). Discovery of a Novel Coumarin/Thiazole Chalcone Hybrid as a Potent Dual Inhibitor of Tubulin and Carbonic Anhydrases IX & XII with Promising Anti-Proliferative Activity. *Molecules*, *31*(6), 917.

Shalini, K., Sharma, P. K., & Kumar, N. (2010). Imidazole and its biological activities: A review. *Der Chemica Sinica*, *1*(3), 36-47.

Shokoohi, M., Sedaghatshoar, S., Arian, H., Mokarami, M., Habibi, F., & Bamarinejad, F. (2025). Genetic advancements in breast cancer treatment: a review. *Discover Oncology*, *16*(1), 127.

Wong, K. C. (2015). Review of spectrometric identification of organic compounds.

Xiong, X., Zheng, L. W., Ding, Y., Chen, Y. F., Cai, Y. W., Wang, L. P., ... & Yu, K. D. (2025). Breast cancer: pathogenesis and treatments. *Signal transduction and targeted therapy*, *10*(1), 49.

Xiong, X., Zheng, L. W., Ding, Y., Chen, Y. F., Cai, Y. W., Wang, L. P., ... & Yu, K. D. (2025). Breast cancer: pathogenesis and treatments. *Signal transduction and targeted therapy*, *10*(1), 49.

Yan, T., Zhang, M. M., Deng, X. Y., Imam, M., Ablise, M., & Zhang, W. Y. (2025). Design and synthesis of novel quinoline-chalcone derivatives as dual inhibitors of tubulin polymerization and P-glycoprotein to overcome cisplatin resistance in cervical cancer. *Bioorganic Chemistry*, 109006.

Yang, J., Lv, J., Cheng, S., Jing, T., Meng, T., Huo, D., ... & Wen, R. (2023). Recent progresses in chalcone derivatives as potential anticancer agents. *Anti-Cancer Agents in Medicinal Chemistry-Anti-Cancer Agents)*, *23*(11), 1265-1283.

Youssef, M. F., Hasanen, J. A., Shehata, A. A., Saleh, A. M., Rizzk, Y. W., & Abdallah, A. M. (2026). Discovery of Novel 1, 3, 5-trisubstituted-2-thioxo-imidazole Derivatives as Potential Aromatase Inhibitors: Design, Synthesis, In Vitro Anti-Breast Cancer Screening and Molecular Docking Studies. *Drug Development Research*, *87*(2), e70243.

Zheng, M., Liu, G., Han, Y., Qian, P., Wu, M., Xiang, M., & Zhou, Y. (2025). Synthesis, biological evaluation and mechanism study of a novel indole-pyridine chalcone derivative as antiproliferative agent against tumor cells through dual targeting tubulin and HK2. *European Journal of Medicinal Chemistry*, *282*, 117058.

Zhuang, C., Zhang, W., Sheng, C., Zhang, W., Xing, C., & Miao, Z. (2017). Chalcone: a privileged structure in medicinal chemistry. *Chemical reviews*, *117*(12), 7762-7810.

Appendix

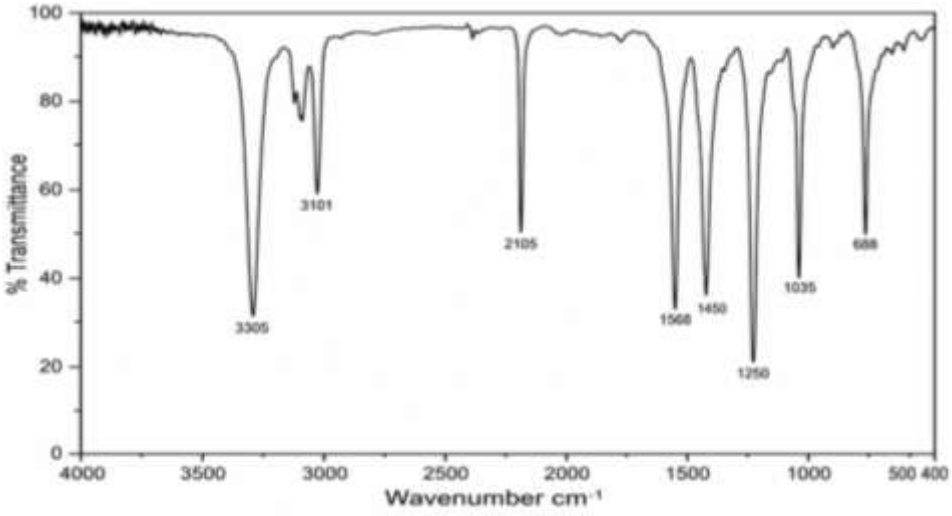

Figure 1: FT-IR spectrum of compound **PI**

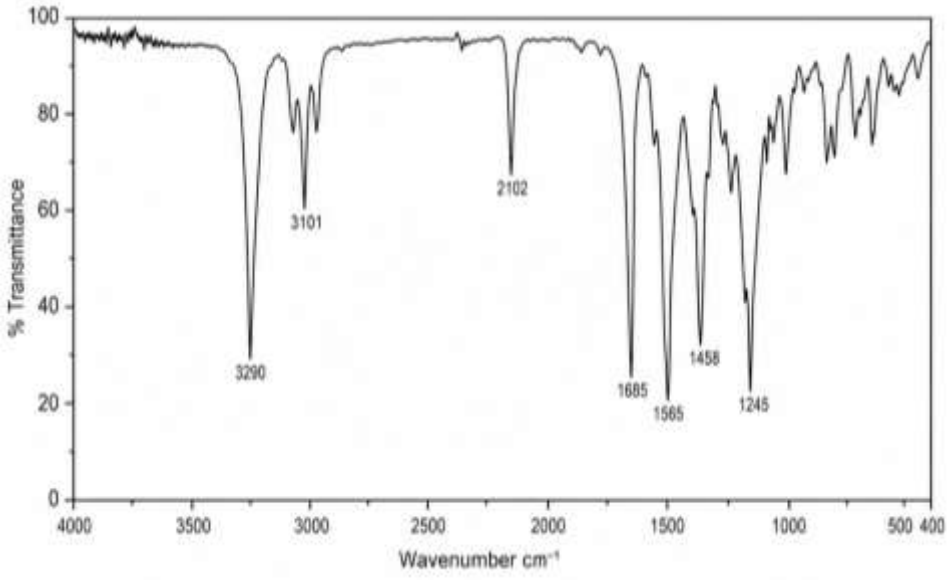

Figure 2: FT-IR spectrum of compound **PIMC**

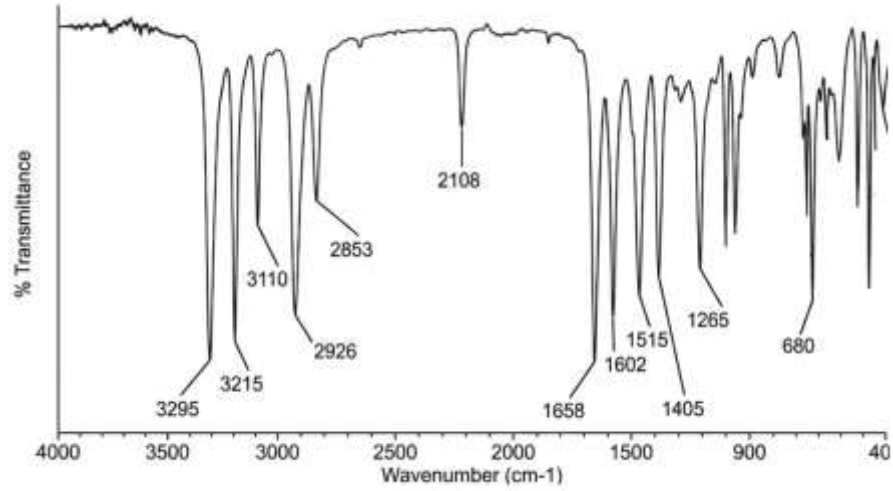

Figure 3: FT-IR spectrum of compound **PIM-1**

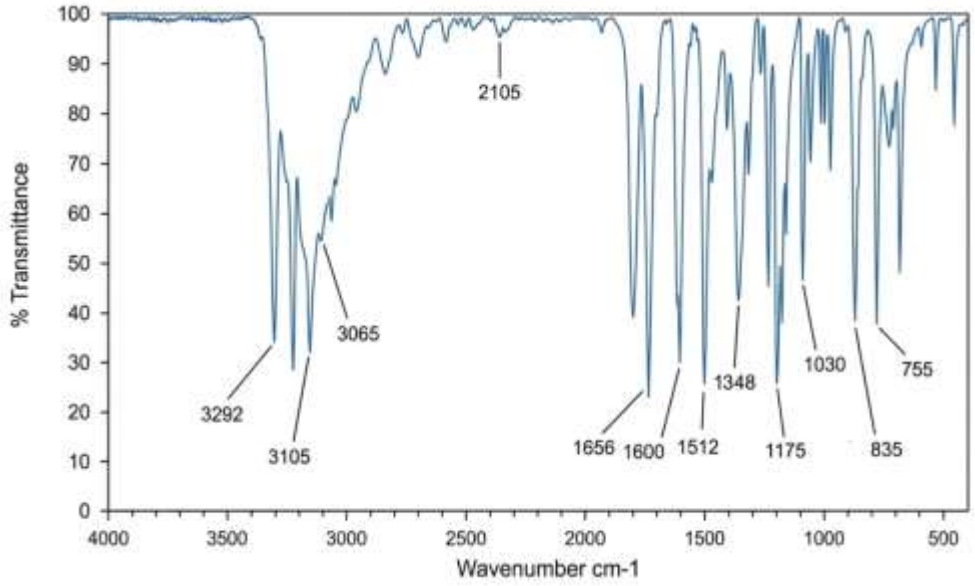

Figure 4: FT-IR spectrum of compound **PIM-2**

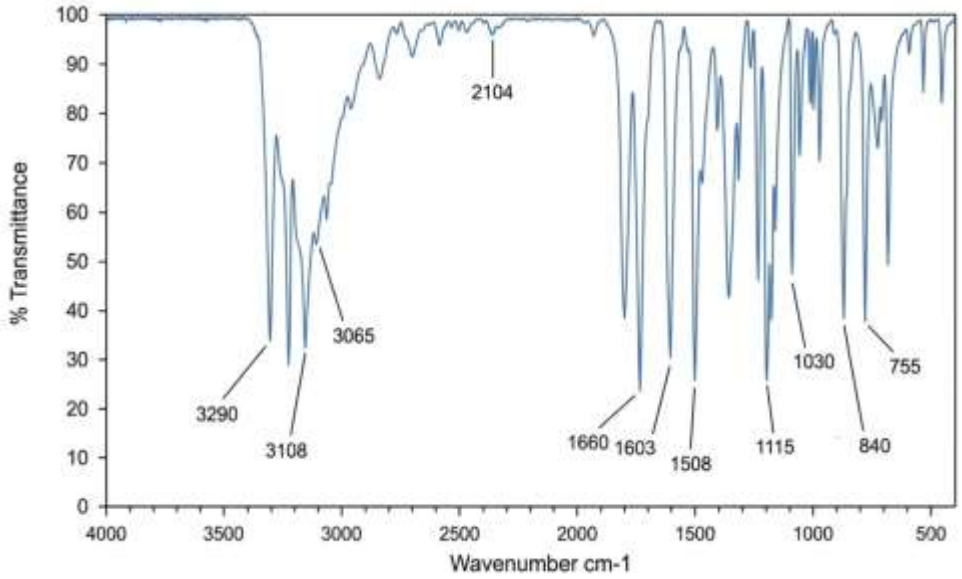

Figure 5: FT-IR spectrum of compound **PIM-3**

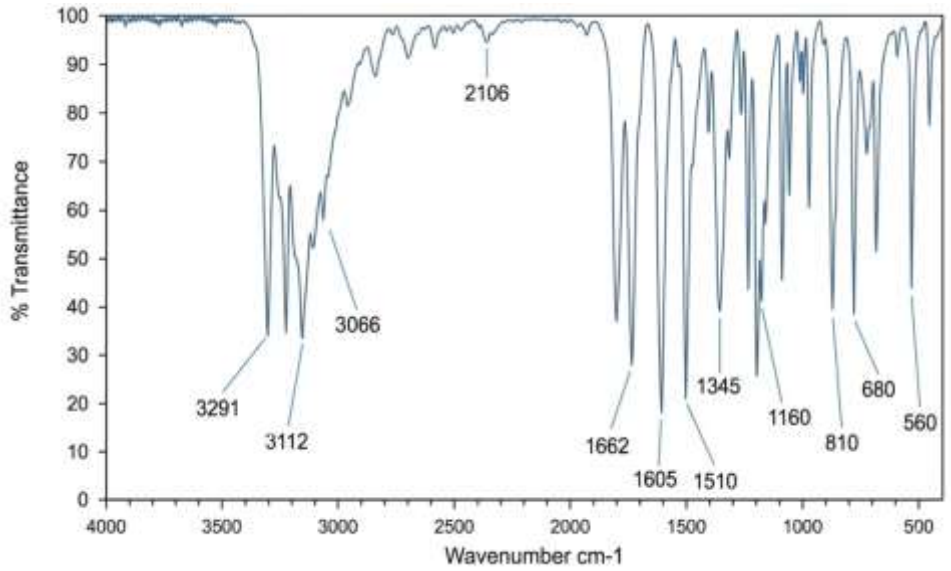

Figure 6: FT-IR spectrum of compound **PIM-4**

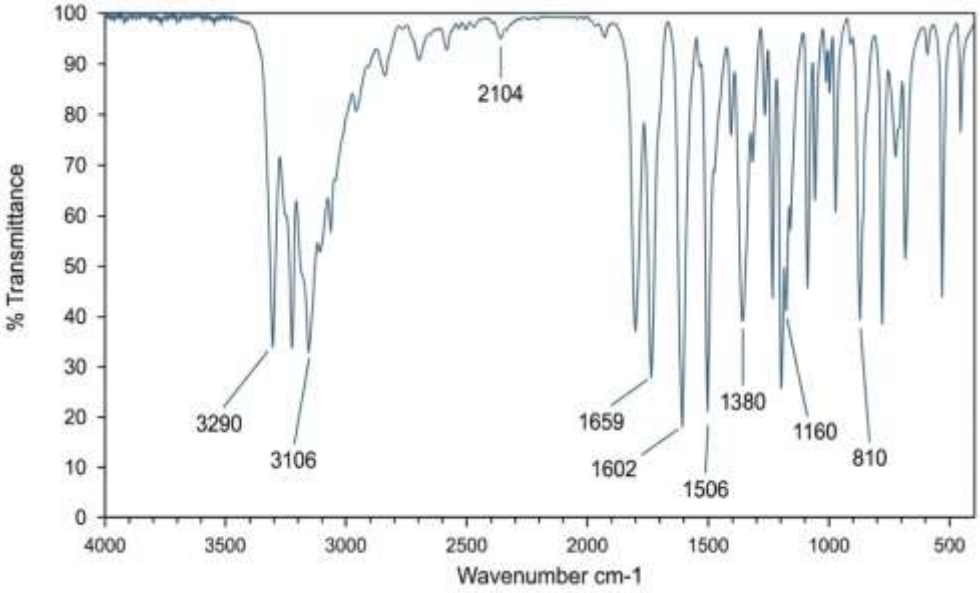

Figure 7: FT-IR spectrum of compound **PIM-5**

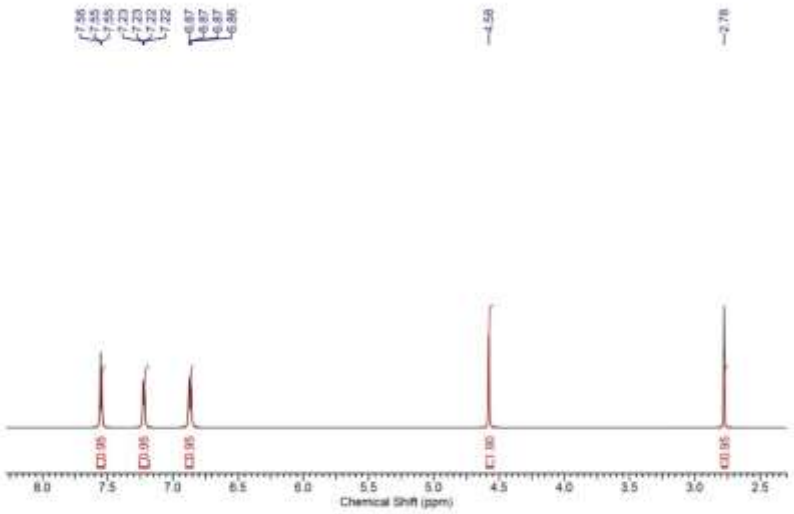

Figure 8: [1]H-NMR spectrum of compound **PI**

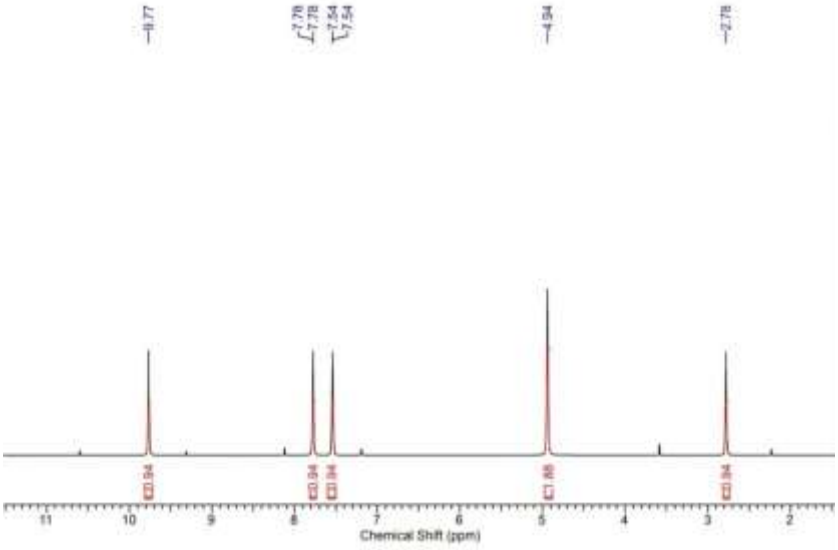

Figure 9: [1]H-NMR spectrum of compound **PIMC**

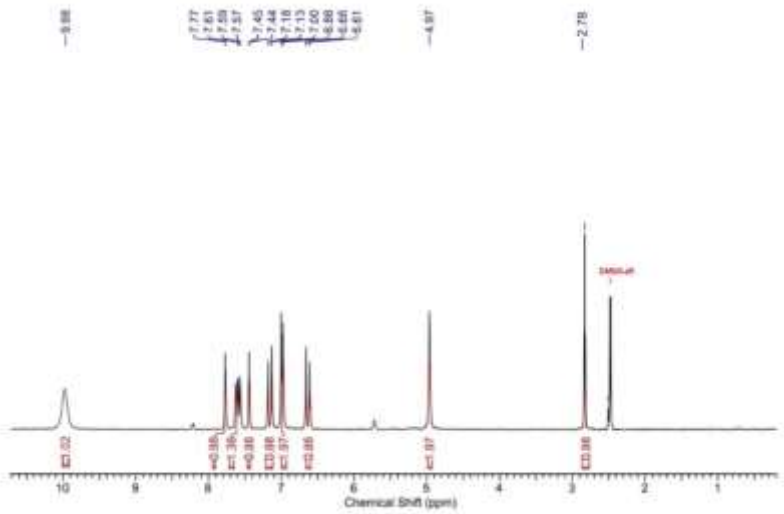

Figure 10: ^{1}H-NMR spectrum of compound **PIM-1**

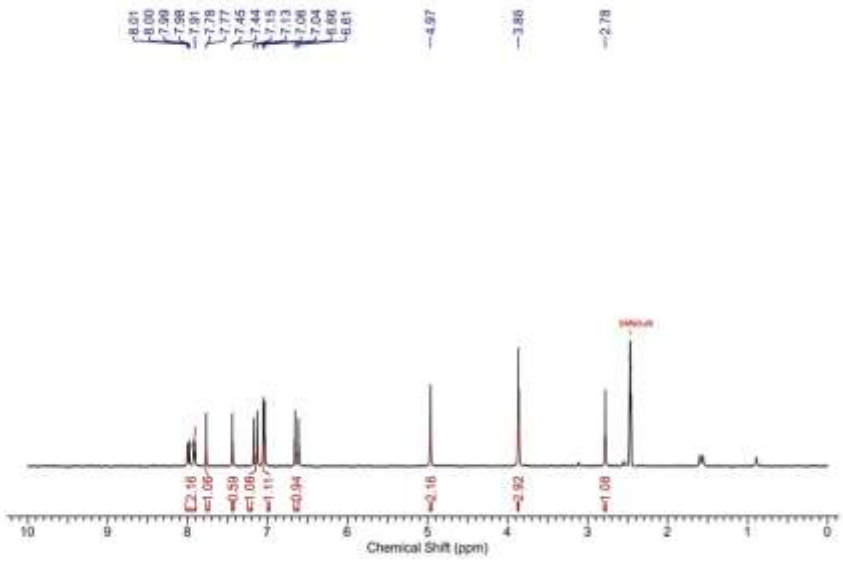

Figure 11: ^{1}H-NMR spectrum of compound **PIM-2**

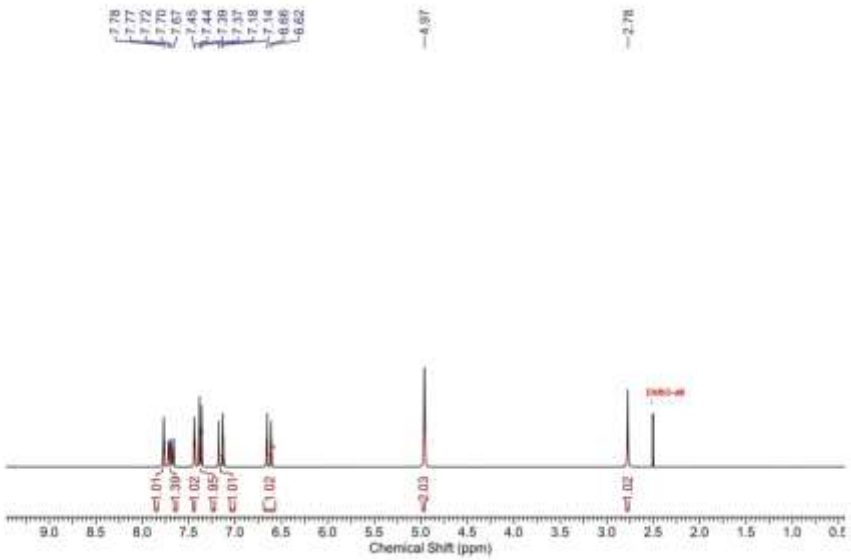

Figure 12: ^{1}H-NMR spectrum of compound **PIM-3**

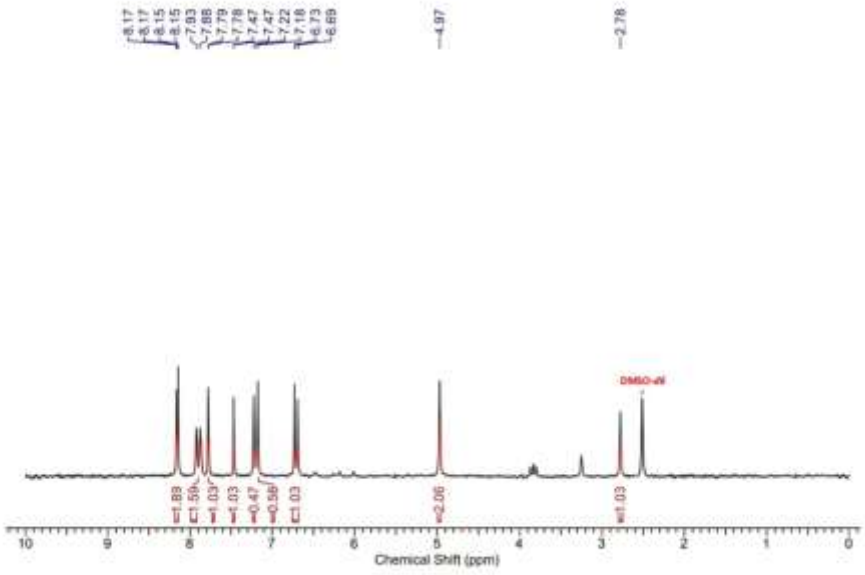

Figure 13: ^{1}H-NMR spectrum of compound **PIM-4**

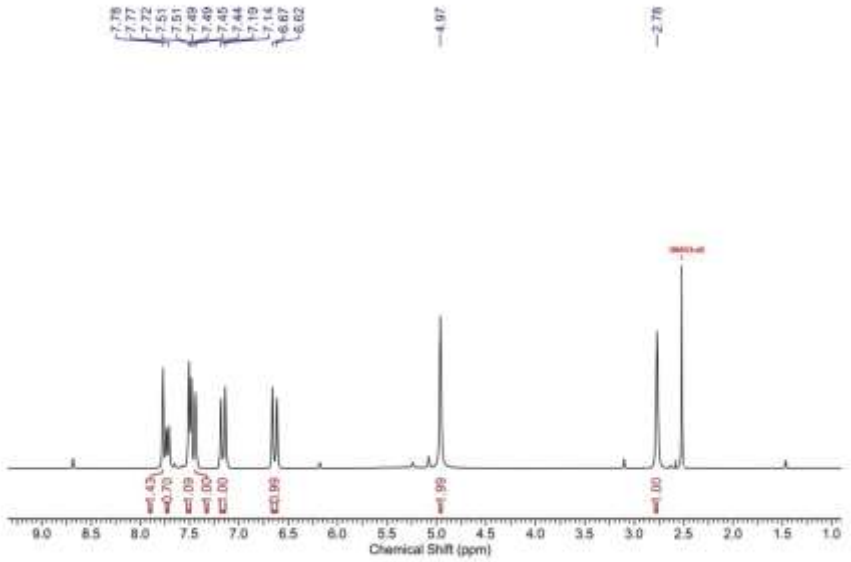

Figure 14: ^{1}H-NMR spectrum of compound **PIM-5**

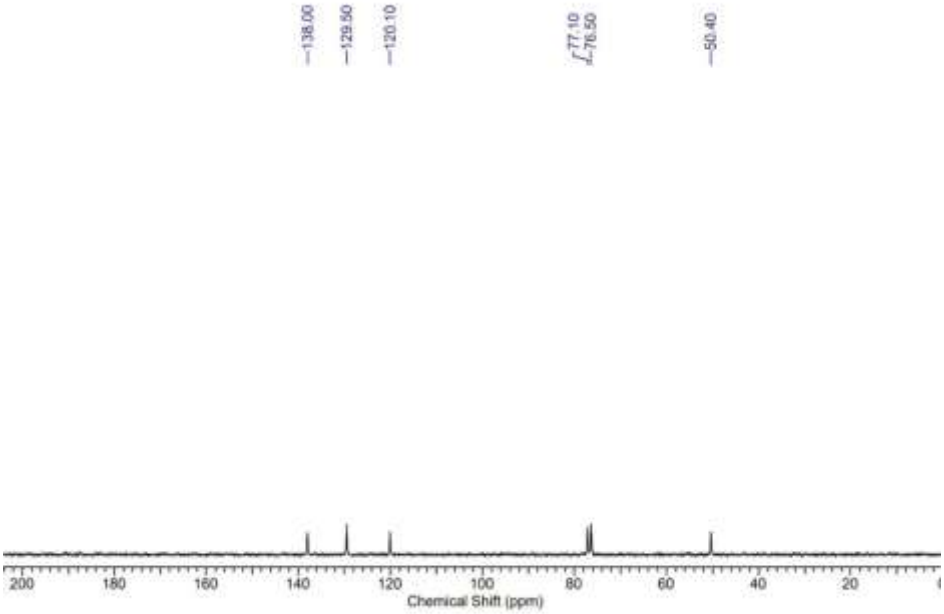

Figure 15: ^{13}C-NMR spectrum of compound **PI**

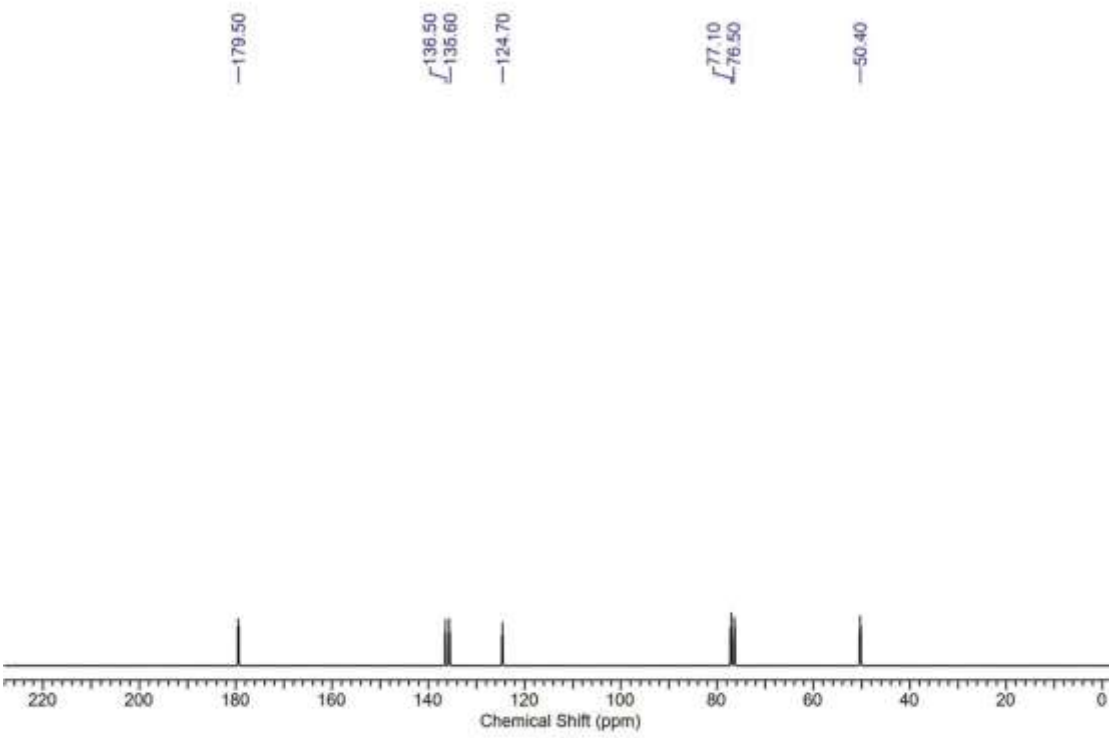

Figure 16: ^{13}C-NMR spectrum of compound **PIMC**

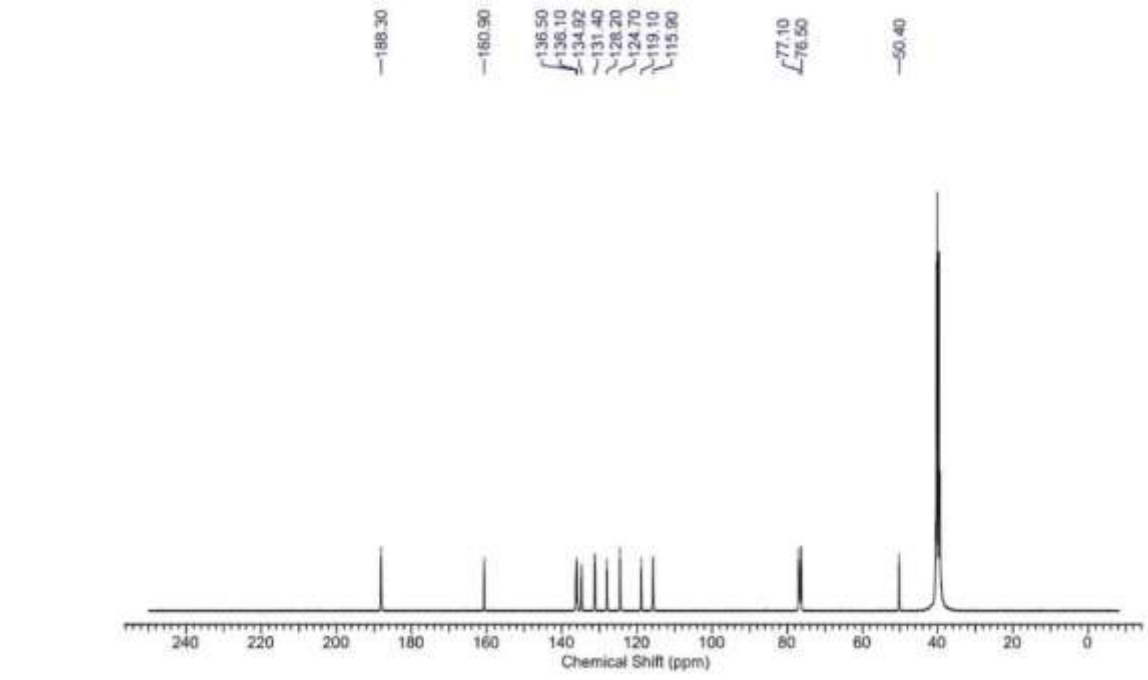

Figure 17: ^{13}C-NMR spectrum of compound **PIM-1**

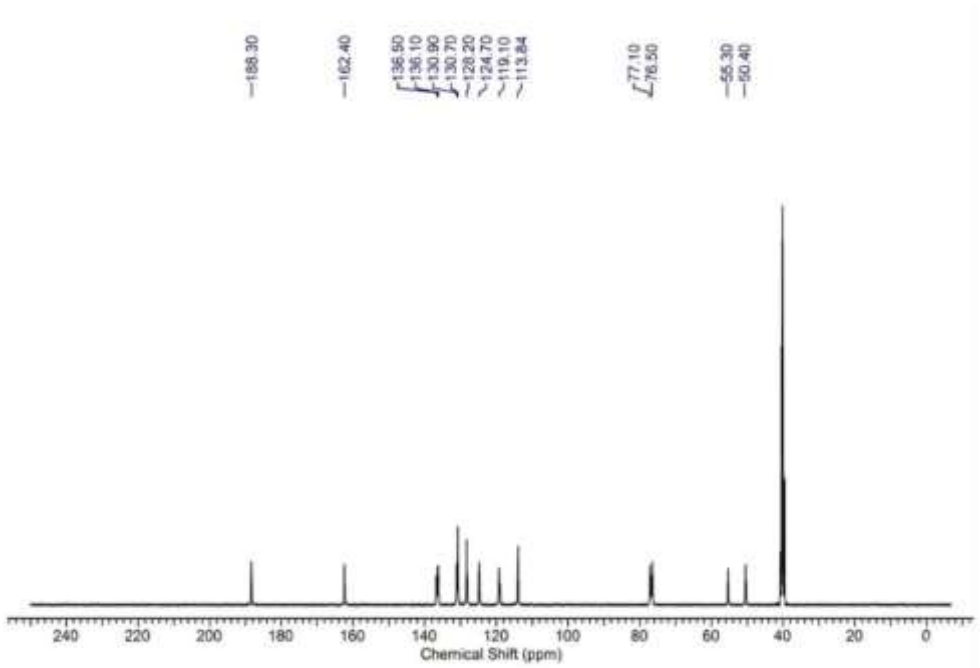

Figure 18: ^{13}C-NMR spectrum of compound **PIM-2**

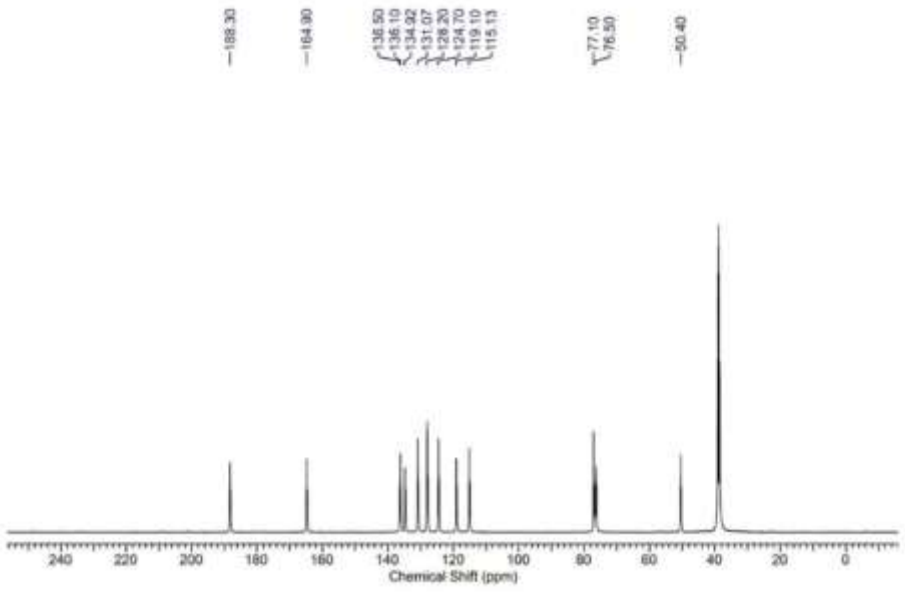

Figure 19: ^{13}C-NMR spectrum of compound **PIM-3**

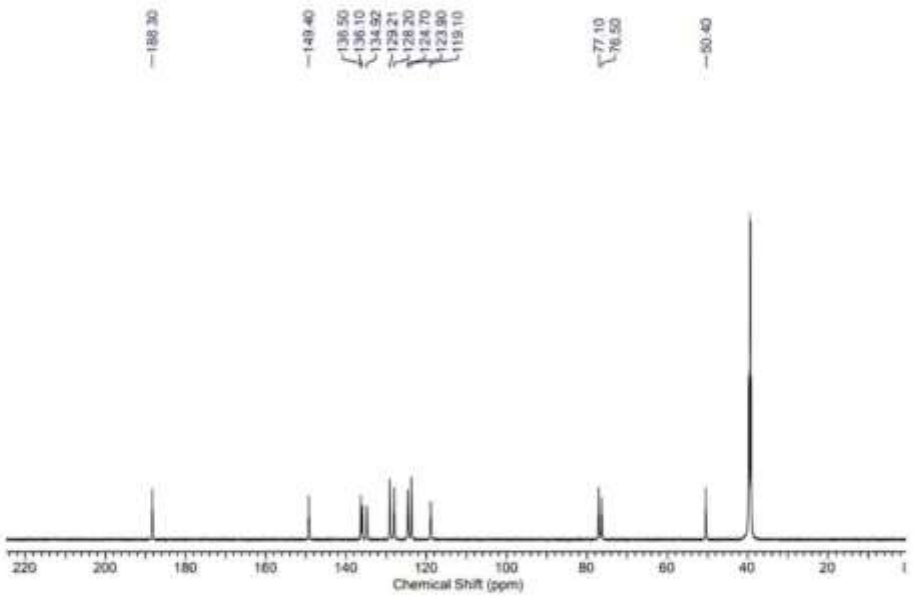

Figure 20: ^{13}C-NMR spectrum of compound **PIM-4**

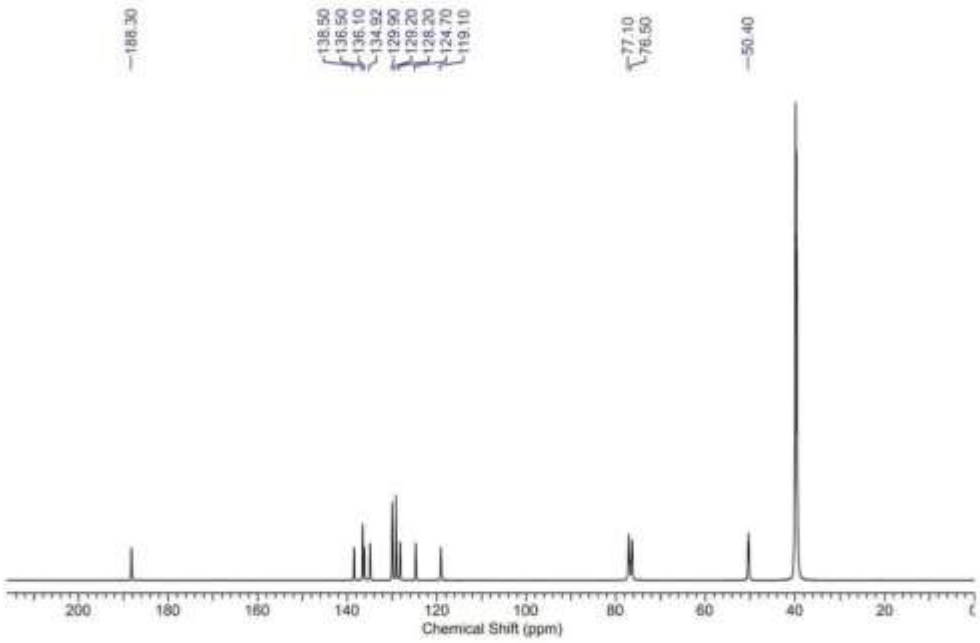

Figure 21: ^{13}C-NMR spectrum of compound **PIM-5**